On the AC Losses in the End Conductors of Hairpin Windings

Marco Pastura, Riccardo Notari, Stefano Nuzzo, Davide Barater, Giovanni Franceschini

Abstract – **In the last years, several resources have been employed to increase torque and power density values in electrical machines, especially in those intended for transport applications. In this context, the adoption of hairpin conductors is spreading thanks to their inherently high fill factor. Their main drawback is represented by their sensitivity to high-frequency phenomena, which can have a significant impact on the Joule losses and thus on the overall efficiency.**

While several researches have recently focused on ways to model and reduce such high-frequency losses in the slots, i.e. within the conductors' active sides, a few data are available on their impact in the end winding regions.

This work provides an investigation on the AC losses occurring in the end conductors of a hairpin winding traction motor. The losses are determined through 3D finite element simulations for a wide frequency range, and compared against those occurring in the active part of the machine.

Index Terms— **End Windings, Hairpin, AC Losses, 3D Finite Element Model**

I. INTRODUCTION

In the last years the research on how to increase torque and power density values of electrical machines, especially for traction application, has led to a major interest for hairpin conductors [1]-[3]. These are pre-formed conductors with a nearly rectangular cross section. They present a higher slot fill factor than classical stranded round conductors, thus also a higher slot thermal conductivity is obtained. These characteristics allow to increase the electrical load without increasing the machine volume, which usually represents a critical constraint for traction applications. In addition, differently from random windings with round conductors, the position of each conductor within the slots is always known and well defined, thus permitting a better modelling and evaluation of the temperature map [4] and of the insulation stress [5].

Hairpin conductors manufacturing can be quite laborious, but can be highly automated, thus fitting the large scale production requirements typical of the automotive sector [6],[7].

However, due to their relatively large cross section, hairpin conductors are quite sensitive to AC losses. The majority of them are caused by skin and proximity effects, which are particularly strong in the machine slots. Depending on their position, slot conductors feature different impedances which result in an uneven current density distribution. This, in turn, also causes an uneven distribution of the Joule losses, which tend to increase from the slot bottom to the air gap. Considering the above, several studies have focused on the modelling and reduction of AC losses [8]-[11], both through analytical and numerical approaches, sometimes also corroborated by experimental measurements. In this context, recent findings in hairpin technologies have demonstrated that the main AC losses reduction techniques include:

- increasing the number of conductors such that a lower cross section and lower conductor current can be adopted. This solution usually requires also a higher number of machine parallel paths [10], [12];

- adoption of variable cross sections, through the use of asymmetric or segmented slot conductors [11], [13]. These solutions consist of having thinner conductors near the air gap and larger ones at the slot bottom. The larger conductors are adopted to decrease the overall DC losses, while thinner conductors are needed to reduce the impact of skin and proximity effects near the slot opening at high frequency operations;

- adoption of different materials than copper, such as aluminium [14], [15]. In fact, AC losses also depend on the material resistivity. Higher resistivity materials increase DC losses, but help in decreasing the frequency dependent effects. The adoption of aluminium can be interesting also for its lower cost, weight and environmental impact, which are all important aspects nowadays.

It is worth mentioning that some of the above solutions may complicate the manufacturing process. Increasing the number of parallel paths and conductors is not always feasible and can increase the manufacturing costs. The adoption of segmented conductors also increases the number of conductors and can be challenging if more than 2 conductors are used to segment an equivalent hairpin layer. Using conductors with different cross sections implies the use of I-pins which, in turn, doubles the number of welding points.

Hairpin windings have to satisfy some mandatory constraints for a proper realization which are strictly linked to the winding topology, the number of slots, poles and conductors. A proper conductor transposition is mandatory every time parallel paths are adopted in order to avoid internal current recirculation, which would increase the Joule losses and decrease the machine performance. These aspects have

M. Pastura, R. Notari, S. Nuzzo, D. Barater and G. Franceschini are with the Department of Engineering "Enzo Ferrari", University of Modena and Reggio Emilia, Modena, Italy (e-mail: marco.pastura@unimore.it; stefano.nuzzo@unimore.it; riccardo.notari@unimore.it davide.barater@unimore.it; giovanni.franceschini@unimore.it).

led, up to now, to consider only integer slot distributed windings, mainly with a full pitch being implemented. Some guidelines for appropriate conductor connections are available in [10], [16]-[18].

A. Motivation and Aim

As inferred in the previous section, the majority of the studies available in literature have focused on the modelling and reduction of AC losses in the active part of machines, while few works have dealt with the end winding regions. In [19] and [20], the end winding leakage inductances are investigated, while in [4] and [21] their cooling is analyzed through oil spray. To the authors' knowledge, only in [22] and [23] the total machine Joule losses are analyzed and the end windings AC losses are considered separately. The results indicate that for a few hundreds of Hertz the end winding losses are nearly DC only, while the frequency dependent effects can become much more relevant around the 1 kHz range. However, a critical analysis on the end windings is missing and the impact of AC losses in the relevant regions is provided for a few values of the frequency. Hence, this work proposes an analysis of the AC losses in the end winding regions for a wide frequency range and their comparison against losses occurring in the machine active part.

II. CASE STUDY

A. Winding Data

The analysis is performed taking as a case study the stator of an electrical machine designed for traction applications. This stator is equipped with a double three-phase (DTP) hairpin winding. The main data of the winding are provided in Table I, while a 2D representation of one stator pole pitch can be seen in Fig. 1. Each slot presents two bigger conductors (namely "conductor 2", see Table I) in the slot bottom such that the DC losses can be decreased avoiding an exacerbation of the frequency dependent losses. The remaining conductors (namely "conductor 1", see Table I) have smaller radial dimensions such that the AC/DC loss ratio remains sufficiently low for the considered frequency
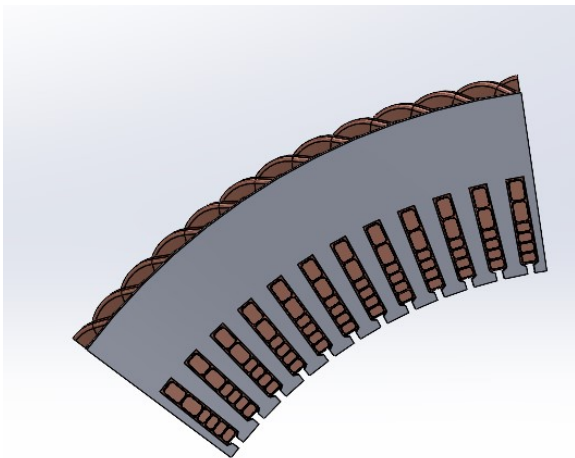
TABLE I. WINDING PARAMETERS

Winding topology	DTP Full Pitch
Slots	96
Number of poles	8
Number of slot conductors	6
Dimensions of conductor 1 [mm]	2.8 x 1.8
Dimensions of conductor 2 [mm]	2.8 x 4

range.

The preliminary sizing of the conductor dimensions is performed according to the theoretical model illustrated in [24], and then validated with finite element analysis (FEA). Depending on the conductor dimensions, material and operating frequency, it is possible to estimate the AC/DC loss ratio (K_{ac}) for every winding layer. A brief summary of the adopted theoretical assumptions and formulas can be found in [15], while more details can be found in [24].

The winding dimensions are optimally selected for a frequency range going from standstill to ≈850 Hz, with a maximum operating frequency of 1 kHz. The conductor dimensions should guarantee a low DC resistance and a winding average K_{ac} below 2 even at 1 kHz. Figure 2 illustrates the trend of K_{ac} for each layer Li (with i=1, 2, …, 6) for the whole frequency range obtained with 2D FEA simulations. K_{ac} is a useful parameter to understand the entity of the frequency dependent losses, since it quantifies how much the losses are higher compared to the DC case. However, in some cases it could be beneficial to have a slightly higher K_{ac}, but a lower DC resistance. This is in fact the case of the first two conductors of the analyzed machine, L1 and L2, which are numbered starting from the slot bottom. The increasing of the K_{ac} is proportionally lower with respect to the reduction of the DC resistance for them.

B. 3D FEA Model

While a 2D model is sufficient to calculate the Joule losses occurring in the active sides of the machine conductors, a 3D model is needed to determine them within the end winding regions.

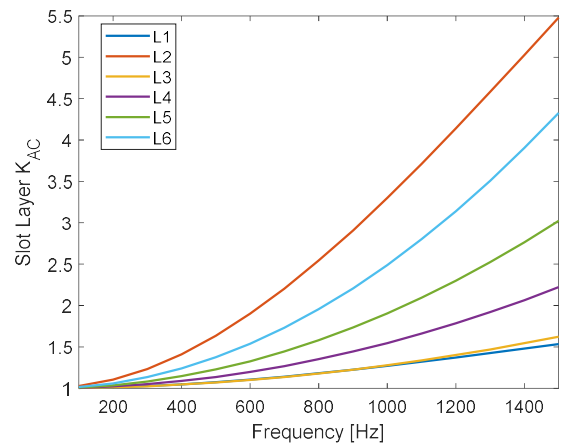
Fig. 1. 2D stator sector of the considered machine.

Fig. 2. AC/DC loss ratio K_{ac} for each layer as a function of frequency. The layer L1 is the one in the slot bottom.

First, a winding scheme is hypothesized and then, basing on it, the end windings are modelled though the CAD-based software Solidworks, where connections and conductor transpositions are opportunely built, as it can be seen in Fig. 3 and Fig. 4. As opposed to 2D FEA electromagnetic modelling, 3D FEA simulations are quite laborious and can take a huge amount of time, thus some measures and assumptions are adopted to speed up the process. These include:

- only 1/8 of the machine is modelled, thus exploiting its periodicity as much as possible;

- since the aim is to study the entity of AC losses in the end windings, the active length can be reduced without affecting the end winding losses;

- the rotor influence on AC losses in the machine active part is somewhat present, but it is also usually quite limited as long as the machine is not highly saturated. Hence, being the end windings surrounded by air, the rotor can be neglected, allowing to further reduce the computation burden. In addition, it allows the adoption of the time harmonic simulations rather than transient with motion ones, which would require much more time
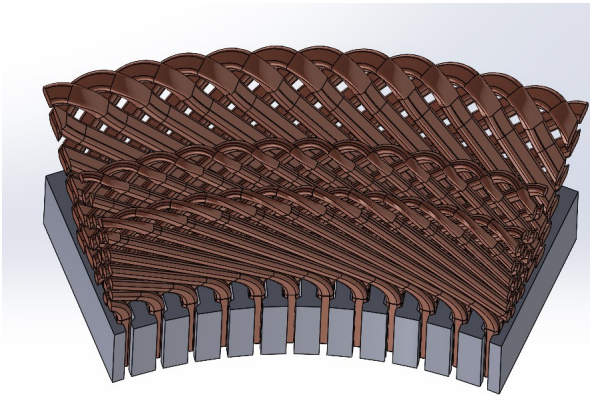

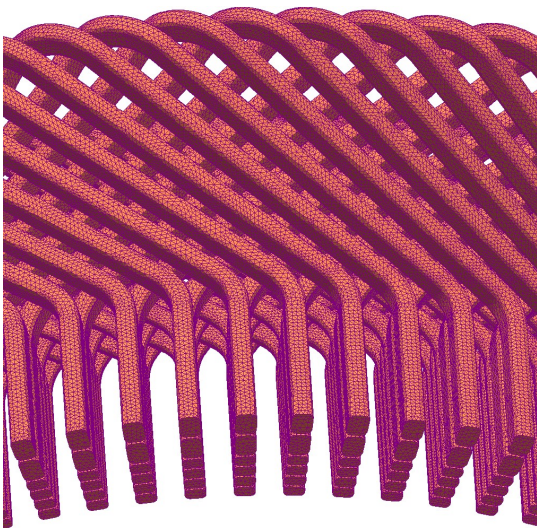Fig.3. 3D model of the machine sector. Front view.

Fig.4. 3D model on the winding. The mesh is also displayed.

to be solved;

- only the end winding insertion side is modelled. Apart from the welding spots, hairpin winding end region sides are rather similar, and a similar behavior can be assumed in terms of AC losses. However, the insertion side tends to be slightly more compact, thus it is the one where a slightly higher impact of the proximity losses is expected.

III. SIMULATION RESULTS

Two types of FEA simulations are performed in the 2D and 3D models: 1) static simulations are carried out to evaluate DC losses and 2) time harmonic simulations are performed to evaluate AC losses as a function of frequency. The frequency range varies from DC to 1500 Hz, which covers the whole automotive typical operating range. All the simulations are run imposing sinusoidal currents feeding the phases, while the conductor material is pure copper with a temperature of 120°C. This operating temperature is separately estimated using a FEA thermal analysis, whose results are out of the scope of this paper, thus they are not reported here. The simulations have been performed also for two opposite case studies: with low saturation (LS) and with high saturation (HS) where the ferromagnetic material has been replaced with a lower permeability material.

The method to isolate the end winding region losses is quite straightforward. Once 3D and 2D simulations have been performed, the end winding losses, P_{ew}, can be estimated using (1) for both static and time harmonic simulations. The term P_{2D} represents only the active length Joule losses, which can be estimated with both 2D simulations or with 3D simulations on a model with only the active part.

$$P_{ew} = P_{3D} - P_{2D} \qquad (1)$$

An important aspect regards the estimation of the end winding AC/DC loss ratio K_{ac}. Nearly all the connections are between the following layers: layers 1 and 2, layers 3 and 4, and layers 5 and 6 as underlined in [16]-[18]. There are a few exceptions, provided by the jumpers, which can connect layers 2 and 3 or layers 4 and 5, but their number is much lower and is kept usually as low as possible. In addition, they are not present in correspondence of all the machine poles. In the considered machine sector, no jumpers are modelled, thus three main types of connection are considered in the end winding of the modelled part. For this reason, three different K_{ac} can be evaluated, depending on which layers' connection is considered (i.e. L1-L2, L3-L4, L5-L6).

Figure 5 illustrates the different values of K_{ac}, depending on the connected layers for the end winding region, while Fig. 6 shows the 2D (active length) counterpart, where the average K_{ac} every two layers (ETL) is evaluated for the sake of comparison. From the theory illustrated in [15] and [24], it is known that the value of K_{ac} for each layer is strictly linked mainly to the operating frequency, conductor radial dimension and the position of the layer. In Figures 5 and 6, it

can be seen that, in the end winding region, the impact of the layer position is lower but still exists. In fact, the lower K_{ac} occurs in both cases for the conductors of L3-L4, which have the same dimensions as those of L5-L6.

Fig. 7 provides a comparison in terms of the average K_{ac} between the end windings and the active part. Fig.7 can be useful to provide a comprehensive overview of the entity of AC losses in the entire end region. It can be seen that, for the maximum frequency of 1500 Hz and LS, a value of 1.26 is nearly obtained. However, in the range from 0 to 900 Hz, the average value is always below 1.1 and with a value of only 1.05 at 650 Hz. In the active part it has a value of 2.9, 1.9 and 1.23 respectively at 1500 Hz, 1000 Hz and 500 Hz. It can be noted also that the K_{ac} curves during conditions of HS are always similar to the ones of LS, but slightly lower values are obtained. In fact, the maximum average K_{ac} is 1.2 at 1.5 kHz for the end winding region and 2.61 for the active one. Thus, the core saturation has also some influence on the end winding region and determines a reduction of the AC losses as in the active part, even if the impact seems quite limited.

While the obtained results are strictly related to the specific design of the considered case study, the findings suggest that the end winding losses can be at first
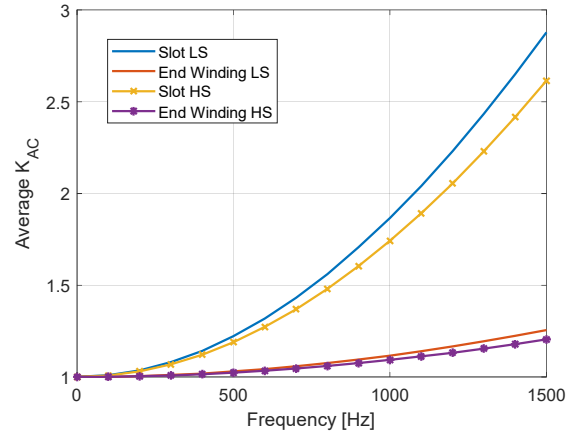

Fig. 7. Comparison of the average value of K_{ac} for the entire end region and active part of the winding.
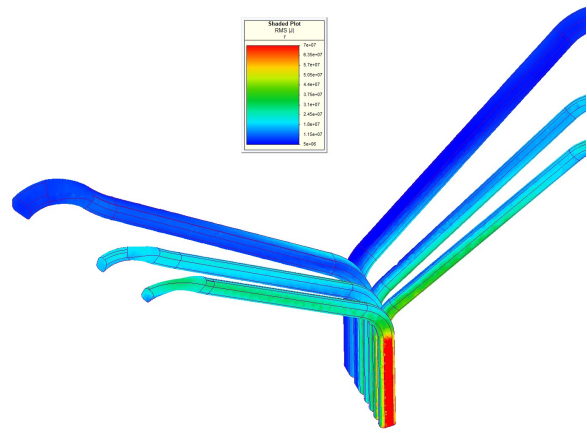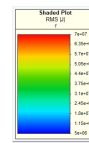

Fig. 8. RMS value of the current density in the conductors of a single slot at 1500 Hz for LS.
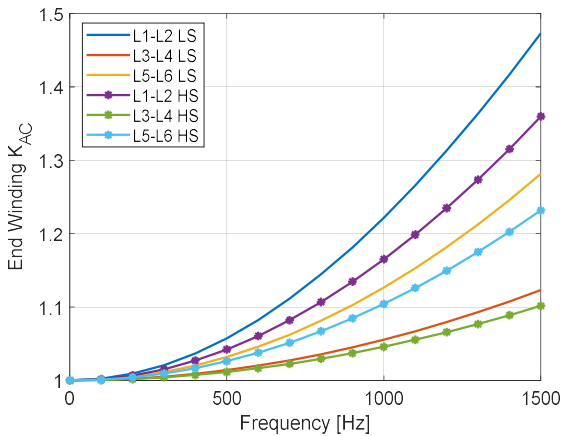

Fig. 5. End winding K_{ac} as a function of frequency for the three different connections.
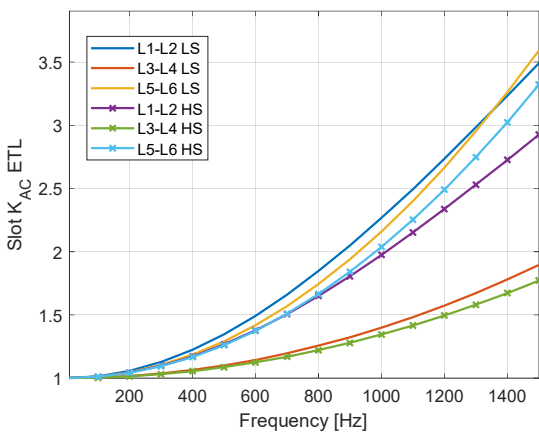
Fig. 6. Active length K_{ac} every two layers as a function of frequency.

approximated as frequency-independent for a considerable frequency range with an acceptable error. In fact, for the considered worst case scenario (LS), K_{ac} in the end winding region exceeds 1.1 only when K_{ac} approaches 1.7 in the active part, which occurs above 900 Hz. For higher values, this approximation could start to be unacceptable, as it can be seen also in Fig. 8. Fig. 8 illustrates the current density map for the conductors of a single slot at the maximum evaluated frequency of 1500 Hz and LS. It can be noted that the values are significantly higher in the active part, however the current displacement is still visible also in the end winding due to the relatively high frequency. In particular, as quantified in Fig. 5, the higher values are obtained in the conductors of the layers 5 and 6.

Further details can be provided by Fig. 9 and Fig.10, where the current density and the flux density are plotted as a function of the radial position for two locations: in the middle of the active part and the at the beginning of the end winding region, at a distance of only 2 mm from the active part. Quite similar results are obtained for both LS and HS, thus only the curves for LS are shown. It can be noted that, in the first part of the end winding region, where the border effects are high, the current density distribution is still pronounced, even if much lower peak values are obtained
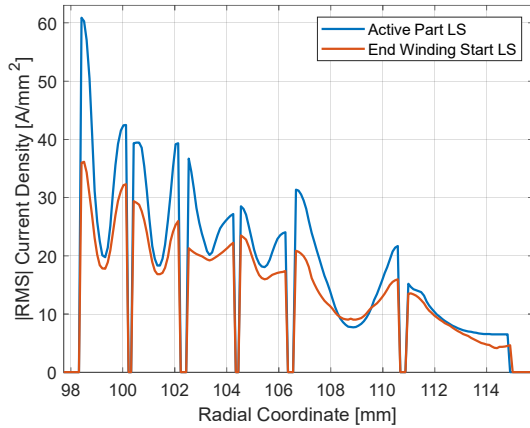
Fig. 9. RMS value of the current density in the conductors of a single slot at 1500 Hz as function of the radial coordinate for LS.
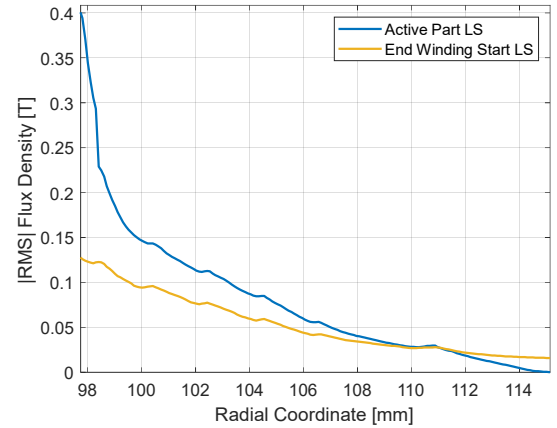

Fig. 10. RMS value of the flux density as function of the radial coordinate for LS.

with respect to the active region. Fig. 10 is instead useful to understand better the previous results. The |B| curve has in fact the same trend for the active part and the end winding region, with the main difference that in the end region it is flatter. The value of |B| is directly linked to the proximity effects, which are stronger where there is a higher a value, while the K_{ac} depends mainly on the proximity effects and conductor radial dimensions. For this reason, in the end winding L3-4 experiments again lower values with respect to the L5-6 since they have the same dimensions, but are still subjected to different |B|. On the other hand, L1-2 has a higher K_{ac} due to its much bigger radial dimension, which has proportionally a higher impact when the |B| distribution is more even.

IV. CONCLUSION

This work focused on the analysis of the AC losses occurring in the end winding regions of a hairpin winding machine through 3D FEA simulations. The modelling approach and the main assumptions to reduce the computation burden for the 3D analysis were illustrated in detail, given their relevance for the sake of this research. The AC/DC loss ratio K_{ac} was evaluated for the different layer connections in the end windings, and its average value was compared also with the one occurring in the active part for a wide frequency range (up to 1.5 kHz). It was observed that the layers involved in one of the connections still have some influence on K_{ac} also in the end windings, though with a much lower impact than in the active part of the machine. Additionally, it was proven that the end winding region exhibits low values of K_{ac} for several hundreds of hertz, allowing to approximate the losses as pure DC with a relatively low error (<10 %), while this approximation is no longer reasonable when approaching 1 kHz.

Future work will focus on analyzing other machine topologies and/or other end winding shapes, with the aim of generalizing the approach and of providing design recommendations related to the end conductors of hairpin windings. Some prototypes will be also built to validate the developed FEA models and the main findings of this paper.

V. ACKNOWLEDGMENT

VI. REFERENCES

[1] Y. Zhao, D. Li, T. Pei and R. Qu, "Overview of the rectangular wire windings AC electrical machine," in CES Transactions on Electrical Machines and Systems, vol. 3, no. 2, pp. 160-169, June 2019, doi: 10.30941/CESTEMS.2019.00022.

[2] S. Nuzzo, D. Barater, C. Gerada and P. Vai, "Hairpin Windings: An Opportunity for Next-Generation E-Motors in Transportation," in IEEE Industrial Electronics Magazine, doi: 10.1109/MIE.2021.3106571.

[3] F. Momen, K. Rahman and Y. Son, "Electrical Propulsion System Design of Chevrolet Bolt Battery Electric Vehicle," in IEEE Transactions on Industry Applications, vol. 55, no. 1, pp. 376-384, Jan.-Feb. 2019, doi: 10.1109/TIA.2018.2868280.

[4] F. Zhang et al., "A Thermal Modeling Approach and Experimental Validation for an Oil Spray-Cooled Hairpin Winding Machine," in IEEE Transactions on Transportation Electrification, vol. 7, no. 4, pp. 2914-2926, Dec. 2021, doi: 10.1109/TTE.2021.3067601.

[5] X. Ju et al., "Voltage Stress Calculation and Measurement for Hairpin Winding of EV Traction Machines Driven by SiC MOSFET," in IEEE Transactions on Industrial Electronics, doi: 10.1109/TIE.2021.3116577.

[6] F. Wirth, T. Kirgör, J. Hofmann and J. Fleischer, "FE-Based Simulation of Hairpin Shaping Processes for Traction Drives," 2018 8th International Electric Drives Production Conference (EDPC), Schweinfurt, Germany, 2018, pp. 1-5, doi: 10.1109/EDPC.2018.8658278.

[7] C. Du-Bar, A. Mann, O. Wallmark and M. Werke, "Comparison of Performance and Manufacturing Aspects of an Insert Winding and a Hairpin Winding for an Automotive Machine Application," 2018 8th International Electric Drives Production Conference (EDPC), Schweinfurt, Germany, 2018, pp. 1-8.

[8] E. Preci et al., "Hairpin Windings: Sensitivity Analysis and Guidelines to Reduce AC Losses," 2021 IEEE Workshop on Electrical Machines

Design, Control and Diagnosis (WEMDCD), 2021, pp. 82-87, doi: 10.1109/WEMDCD51469.2021.9425643.

[9] P. S. Ghahfarokhi, A. Podgornovs, A. J. Marques Cardoso, A. Kallaste, A. Belahcen and T. Vaimann, "Hairpin Windings Manufacturing, Design, and AC Losses Analysis Approaches for Electric Vehicle Motors," 2021 11th International Electric Drives Production Conference (EDPC), 2021, pp. 1-7, doi: 10.1109/EDPC53547.2021.9684208.

[10] G. Berardi, N. Bianchi, "Design guideline of an AC hairpin winding", 2018 XIII International Conference on Electrical Machines (ICEM), pp. 2444-2450, 3.-6. Sept. 2018.

[11] E. Preci et al., "Segmented Hairpin Topology for Reduced Losses at High Frequency Operations," in IEEE Transactions on Transportation Electrification, doi: 10.1109/TTE.2021.3103821.

[12] M. Pastura, D. Barater, S. Nuzzo and G. Franceschini, "Multi Three-Phase Hairpin Windings for High-Speed Electrical Machine: Possible Implementations," 2021 IEEE Workshop on Electrical Machines Design, Control and Diagnosis (WEMDCD), 2021, pp. 113-118, doi: 10.1109/WEMDCD51469.2021.9425640.

[13] M. S. Islam, I. Husain, A. Ahmed and A. Sathyan, "Asymmetric Bar Winding for High-Speed Traction Electric Machines," in IEEE Transactions on Transportation Electrification, vol. 6, no. 1, pp. 3-15, March 2020.

[14] A. Acquaviva, M. Diana, B. Raghuraman, L. Petersson and S. Nategh, "Sustainability Aspects of Electrical Machines For E-Mobility Applications Part II: Aluminium Hairpin vs. Copper Hairpin," IECON 2021 – 47th Annual Conference of the IEEE Industrial Electronics Society, 2021, pp. 1-6, doi:10.1109/IECON48115.2021.9589649.

[15] M. Pastura, D. Barater, S. Nuzzo and G. Franceschini, "Investigation of Resistivity Impact on AC Losses in Hairpin Conductors," IECON 2021 – 47th Annual Conference of the IEEE Industrial Electronics Society, 2021, pp. 1-6, doi: 10.1109/IECON48115.2021.9589047.

[16] S. Zhu, K. Paciura and R. Barden, "Design Approach of Hairpin Winding Motor with High Parallel Path Numbers," 2021 IEEE Energy Conversion Congress and Exposition (ECCE), 2021, pp. 4534-4538, doi: 10.1109/ECCE47101.2021.9595449.

[17] M. England, B. Dotz and B. Ponick, "Evaluation of Winding Symmetry and Circulating Currents of Hairpin Windings," 2021 IEEE International Electric Machines & Drives Conference (IEMDC), 2021, pp. 1-8, doi: 10.1109/IEMDC47953.2021.9449604.

[18] T. Zou et al., "A Comprehensive Design Guideline of Hairpin Windings for High Power Density Electric Vehicle Traction Motors," in IEEE Transactions on Transportation Electrification, doi: 10.1109/TTE.2022.3149786.

[19] S. Moros, J. Kempkes and S. Tenner, "Numerical Calculation of End-Coil'S Leakage Inductance for Concentrated and Hairpin Windings," 2019 IEEE International Electric Machines & Drives Conference (IEMDC), 2019, pp. 1144-1150, doi: 10.1109/IEMDC.2019.8785365.

[20] M. Silberberger, D. P. Morisco, H. Rapp and A. Möckel, "Calculation of end-winding leakage inductance for hairpin winding high power density traction machines using the PEEC method," 2021 IEEE International Electric Machines & Drives Conference (IEMDC), 2021, pp. 1-7, doi: 10.1109/IEMDC47953.2021.9449550.

[21] C. Liu et al., "Experimental Investigation on Oil Spray Cooling With Hairpin Windings," in IEEE Transactions on Industrial Electronics, vol. 67, no. 9, pp. 7343-7353, Sept. 2020, doi: 10.1109/TIE.2019.2942563.

[22] M. Aoyama and J. Deng, "Visualization and quantitative evaluation of eddy current loss in bar-wound type permanent magnet synchronous motor for mild-hybrid vehicles," in CES Transactions on Electrical Machines and Systems, vol. 3, no. 3, pp. 269-278, Sept. 2019, doi: 10.30941/CESTEMS.2019.00035.

[23] H. Sano, T. Aasanuma, H. Katagiri, M. Miwa, K. Semba and T. Yamada, "Loss calculation of bar-wound high-power-density PMSMs with massively parallel processing," 2017 IEEE International Electric Machines and Drives Conference (IEMDC), 2017, pp. 1-6, doi: 10.1109/IEMDC.2017.8002252.

[24] J. Pyrhonen, J. Tapani, and V. Hrabovcova,` Design of Rotating Electrical Machines. Chichester, U.K.: Wiley, 2008.

VII. BIOGRAPHIES

Marco Pastura received the M.Sc. degree in Electrical Engineering from the University of Pavia, Pavia, Italy in 2018. He is currently a Ph.D. student in "Automotive Engineering for Intelligent Mobility" at the Department of Engineering "Enzo Ferrari" at University of Modena and Reggio Emilia, Modena, Italy. His research interests are the electrical drives for automotive and aerospace applications with focus on high reliability electrical machines.

Riccardo Notari received the B.Sc. and M.Sc. degrees in Mechanical Engineering from the University of Modena and Reggio Emilia, Modena, Italy, in 2019 and 2021, respectively. Since 2022 he is pursuing a Ph.D. degree with the Mechanical Electrical Engineering (MEltIng) Group, University of Modena and Reggio Emilia. His main research interests are the modelling, analysis and multiphysics optimization of electrical machines and drive

Stefano Nuzzo Stefano Nuzzo (S'17-M'18) received the B.Sc. and M.Sc. degrees in Electrical Engineering from the University of Pisa, Pisa, Italy, in 2011 and 2014, respectively. He received his Ph.D. degree in Electrical and Electronics Engineering in 2018 from the University of Nottingham, Nottingham, U.K, where he also worked as a Research Fellow within the Power Electronics, Machines and Control (PEMC) Group. Since January 2019, he works within the Department of Engineering "Enzo Ferrari" at University of Modena and Reggio, Modena, Italy, where he is a Lecturer in Electrical Machines and Drives. His research interests are the analysis, modelling and optimizations of electrical machines intended for power generations, industrial and transport applications. He is involved in a number of projects related to the more electric aircraft initiative and associated fields. Dr. Nuzzo is a Member of the IEEE Industrial Electronics Society (IES) and the IEEE Industry Applications Society (IAS). He serves as Associate Editor for the IEEE Transactions on Transportation Electrification.

Giovanni Franceschini received the M.Sc. degree in Electronic Engineering from the University of Bologna, Bologna, Italy. He is currently the Full Professor of Electric Drives with the Department of Engineering "Enzo Ferrari", University of Modena and Reggio Emilia, Modena, Italy. He was the Coordinator of the European Project ALEA, to achieve complete and accurate lifetime models for electrical drives in aerospace applications. He is the author or co-author of more than 150 international papers. His research interests include power electronics for e-mobility and motor drives control and diagnostic.

Davide Barater (S'11-M'14) received the M.Sc. degree in Electronic Engineering in 2009 and the Ph.D. degree in Information Technology in 2014 from the University of Parma Italy. He was an honorary scholar at the University of Nottingham, U.K., during 2012, and a visiting researcher at the University of Kiel, DE in 2015. He is currently Associate Professor at Department of Engineering "Enzo Ferrari", University of Modena and Reggio Emilia, Italy. His research area is focused on power electronics for e-mobility and motor drives. He is a Coordinator of the European Project AUTO-MEA that aims to develop electrical motors and drives for next generation of electrical mobility. He is Associate Editor of IEEE Transactions on Industry Applications and author or co-author of more than 60 international papers.